IN SITU ANALYSIS OF THIN FILM DEPOSITION PROCESSES USING TIME-OF-FLIGHT (TOF) ION BEAM ANALYSIS METHODS*

Jaemo Im[1,2], Alan R. Krauss[1], Yuping Lin[3], J. A. Schultz[4], Orlando H. Auciello[5], Dieter M. Gruen[1], and R. P. H. Chang[2]

[1]Materials Science and Chemistry Divisions, Argonne National Laboratory, Argonne, IL 60439
[2]Department of Materials Science and Engineering, Northwestern University, Evanston, IL 60208
[3]QQC, Inc., Dearborn MI 48126
[4]Ionwerks, Houston, TX 77005
[5]MCNC, Electronics Technology Division, Research Triangle Park, NC 27709

Submitted to

Nuclear Instruments and Methods in Physical Research B

May 1995

*Work supported by the U.S. Department of Energy, BES-Materials Sciences, under Contract W-31-109-ENG-38.

Presented at the 12th Ion Beam Analysis Conference, Tempe AZ May 22-26, 1995
Submitted to Nuclear Instruments and Methods in Physical Research B

IN SITU ANALYSIS OF THIN FILM DEPOSITION PROCESS USING TIME OF FLIGHT (TOF) ION BEAM ANALYSIS METHODS*

Jaemo Im[1,2], Alan R. Krauss[1], Yuping Lin[3], J. A. Schultz[4], Orlando H. Auciello[5], Dieter M. Gruen[1], and R. P. H. Chang[2]

1. Material Science and Chemistry Divisions, Argonne National Laboratory, Argonne, IL 60439
2. Dept. of Materials Science and Engineering, Northwestern University, Evanston, IL 60208
3. QQC Corporation,Dearborn MI 48126
4. Ionwerks, Houston TX 77005
5. MCNC, Electronics Technology Division, Research Triangle Park, NC 27709

The use of comprehensive, non-destructive, in situ methods for the characterization of thin film growth phenomena is key both to obtaining a better understanding of thin film growth processes and to the development of more reliable deposition procedures, especially for complex layered structures involving multi-phase materials. However, surface characterization methods that utilize either electrons (e.g. AES or XPS) or low energy ions (SIMS) for the signal require an UHV environment and utilize instrumentation which obstructs line of sight access to the substrate. These methods are therefore incompatible with line of sight deposition methods and thin film deposition processes which introduce gas, either as an intrinsic part of the deposition procedure or in order to produce the desired phase such as an oxide film of a particular crystal structure or stoichiometry. We have developed a means of differentially pumping both the ion beam source and detectors of a TOF ion beam surface analysis spectrometer that does not interfere with the deposition process and permits compositional and structural analysis of the growing film in the present system, at pressures up to several mTorr. Higher pressures are feasible with modified source-detector geometry.

In order to quantify the sensitivity of Ion Scattering Spectroscopy (ISS) and Direct Recoil Spectroscopy (DRS), we have measured the signal intensity for stabilized clean metals in a variety of gas environments as a function of the ambient gas species and pressure, and ion beam species and kinetic energy. The results are interpreted in terms of collision cross sections which are compared with known gas phase scattering data and provide an *apriori* basis for the evaluation of time-of-flight ion scattering and recoil spectroscopies (ToF-ISARS) for various industrial processing environments which involve both inert and reactive gases. The cross section data for primary ion-gas molecule and recoiled atom-gas molecule interactions are also provided, from which the maximum operating pressure in any experimental configuration can be obtained.

* Work supported by the U. S. Department of Energy, Division of Basic Energy Science, under contract W-31-109-ENG-38.

INTRODUCTION

As device structures become increasingly more complex, and multi-component, multi-phase materials come into greater use, the need for in situ monitoring of thin film deposition processes becomes increasingly important. Growth of oxide or nitride films typically requires an ambient atmosphere of oxygen or nitrogen. A number of the more technologically interesting materials exhibit a growth surface that is only kinetically stable [1,2], depending strongly on maintenance of the substrate temperature, oxygen or nitrogen and metal fluxes in a manner which makes ex situ surface analytical methods unsuitable for elucidation of the growth process. Conventional surface analytical methods are not suitable for in situ characterization of thin film growth, both because the analytical instrumentation blocks line of sight deposition, and because the methods require an ultra-high vacuum environment.

Pulsed ion beam surface analysis using primary ions in the 1-100 keV range is capable of characterizing the surface composition and structure with a depth resolution comparable to or better than electron or low energy ion-based surface analytical methods such as Auger, x-ray photoelectron spectroscopy (XPS) or secondary ion mass spectroscopy (SIMS). Measurement of the kinetic energy of the scattered primary ion provides a means of determining the mass of the surface collision partner, M_2. The corresponding surface analytical method is known as ion scattering spectroscopy (ISS). Alternatively, M_2 can be determined by measuring the kinetic energy E_2 of the surface atoms ejected by direct recoil collisions. The corresponding surface analytical method is known as direct recoil spectroscopy (DRS). These methods have been shown to be capable of providing an exceptionally wide range of information on the surface composition and structure [3-7].

The detected species in both ISS and DRS consist of ions or neutral atoms which have kinetic energies of several keV and are therefore not as subject to gas phase scattering as conventional surface analysis methods. In order to provide a means of non-destructive, real-time, in situ, surface-specific analysis which does not interfere with the deposition process and may be operated under conditions dictated by the deposition process rather than the analysis method, we have developed a differentially pumped time of flight ion scattering (ISS) and direct recoil (DRS) spectrometer. This instrument provides monolayer-specific real-time information on the surface composition and structure in ambient atmospheres associated with thin film deposition environments and does not intrude on the deposition line of sight or the space required for thin film deposition equipment.

The work in this paper is concentrated on quantifying the gas phase scattering effects on the ISS and DRS signals at relatively high ambient pressures. In general, it is to be expected that gas phase scattering might result in peak broadening and shift, and signal attenuation, and these effects

might be expected to degrade the usefulness of the data well before the maximum operating pressures of the ion beam source and detectors are reached. A third ToF-ISARS method, that of Mass Spectroscopy of Recoiled Ions (MSRI) [8] is also under investigation for operation under ambient processing conditions, and it appears that MSRI may be even more tolerant of background gas than ISS and DRS.

Collisional cross sections for ISS and DRS signal attenuation are measured for various ion beam-ambient gas conditions, and design data for retrofitting existing thin film deposition systems or designing new Tof-ISARS instruments for in situ, real-time process monitoring are presented.

THEORY

The energy transfer between a primary ion with kinetic energy E_o in the range 1-100 keV and a surface atom with mass M_2 is described by classical two-body collision dynamics. The primary ion with mass M_1 is scattered at an angle θ_1 with energy E_1 given by [9]

$$E_1=E_o\,(1+\alpha)^{-2}\,[\cos\theta_1 \pm (\alpha^2-\sin^2\theta_1)^{1/2}]^2 \qquad (1)$$

where $\alpha=M_2/M_1$. The surface atom may be ejected by a direct recoil collision with a kinetic energy

$$E_2=E_o\,4\alpha\,(1+\alpha)^{-2}\cos^2\theta_2 \qquad (2)$$

where θ_2 is the angle of the recoil particle's trajectory with respect to that of the incident primary ion.

At a given ambient pressure and kinetic energy, the number of energetic particles (scattered primary ions or recoil-sputtered surface atoms) which survive after traveling a given distance d through a gas is given by

$$I= I_0\,e^{-d/\lambda}, \qquad (3)$$

where I_0 is the primary beam intensity in vacuum, c is a constant, and

$$\lambda=kT/p\sigma, \qquad (4)$$

is the collisional mean free path, where k is Boltzmann's constant, T is the temperature, p is the pressure and σ is the collision cross section between the energetic particle and the gas molecules. Therefore the gas phase attenuation is given by

$$I=I_0\,e^{-dp\sigma/kT}. \qquad (5)$$

In the present experiment, we observe the effect of gas phase scattering on the attenuation of both the ion beam incident on the sample and the exit beam from the sample to the detector. The kinetic energy of the exit beam will always be less than that of the primary beam and, in the case of DRS, the mass will also differ from that of the primary beam. Therefore, equation 3 becomes

$$I=I_0\, e^{-p(d_1\sigma_1+d_2\sigma_2)/kT} \qquad (6)$$

where d_1 (0.2845m) and d_2 (0.118 m) are the distances which are traversed through the high pressure region for the incoming and outgoing particles, respectively, σ_1 is the cross section which determines the flux of the primary beam (with initial kinetic energy E_1) arriving at the sample, and σ_2 is the cross section which determines the number of scattered primary ions (eq. 1) or direct recoil surface atoms (eq. 2) arriving in a small solid angle subtended by the detector. σ_2 therefore represents a partial, rather than the total direct recoil cross section. Alternatively, eq. 6 may be rewritten as

$$I=I_0\, e^{-(d_1+d_2)p<\sigma>/kT} \qquad (7)$$

where

$$<\sigma>=\frac{d_1\sigma_1(E_0)+d_2\sigma_2(E_1)}{d_1+d_2} \qquad \text{(ISS)} \qquad (8a)$$

or

$$<\sigma>=\frac{d_1\sigma_1(E_0)+d_2\sigma_2(E_2)}{d_1+d_2} \qquad \text{(DRS),} \qquad (8b)$$

and $<\sigma>$ is a path length-weighted mean cross section. In general, σ_1 and σ_2 depend on the kinetic energy, mass, charge and state of excitation of the incoming and outgoing particles.

EXPERIMENTAL TECHNIQUE

An illustration of the experimental apparatus is shown in Fig. 1. The integrated thin film deposition/surface analysis chamber consists of time of flight ion scattering and direct recoil (ISS, DRS) and Auger electron spectrometers, coupled to a multitarget ion beam sputter deposition system (IBSD). The base pressure of the surface analysis chamber is in the mid 10^{-10} Torr range when pumped by a 200 liter/sec ion pump and Ti sublimation pump. At the relatively high operating pressures associated with the thin film deposition process, a 250 liter/sec turbomolecular pump connected to the load lock chamber is used, with a base pressure in the low 10^{-8} Torr range. A leak valve is used to introduce gases as required for the deposition process. Oxygen, argon, nitrogen and hydrogen were chosen as the background gases in this experiment. The detailed description of the TOF-ISARS and IBSD systems can be found in previous papers [9-10].

The diagram of the present system is shown in Fig. 1. In brief, a telefocus ion source (Atomika W610) is used to produce a highly collimated ion beam with a typical kinetic energy of ~10 keV. The beam passes through two deflection regions, separated from each other by an apertured drift space. By controlling the time interval between the application of voltage steps to the two sets of deflection plates, a pulsed ion beam with pulse duration adjustable from ~10 to 1000 nsec is produced. A final set of dc deflection plates is then used to steer the beam to the desired location on the sample. The beam line is differentially pumped via a 100 l/sec turbomolecular pump located immediately after the ion extractor, and a 70 l/sec turbomolecular pump immediately before the final aperture into the analysis chamber.

Two channel electron multiplier detectors are positioned at angles of 165 and 25 degrees (Fig. 2) relative to the incident beam direction. Each detector views the sample through a 1 mm diameter differential pumping aperture located at the end of a 1.3 cm diameter stalk, terminating 11.2 cm from the sample. Pumping for each detector is provided by a 60 l/sec. turbomolecular pump, and a Bayard-Alpert ion gauge is used to monitor the pressure at the detector. An interlock circuit removes voltage from the detector if the pressure at the detector rises above 2×10^{-5} Torr. Assuming the rated pumping speed for the turbomolecular pump, the corresponding maximum chamber pressure is 12 mTorr.

RESULTS AND DISCUSSION

ISS spectra for 10 keV Ne^+ incident on Au in an Ar ambient are shown as a function of Ar pressure in Fig. 3. The 10 keV beam energy was chosen for reasons of experimental convenience, although comparison data sets acquired with 8 and 12 keV energies do not show significantly different results. Au was chosen as the sample in order to eliminate adsorption effects from the gas ambient. Since there is no adsorption, all changes in the signal attenuation are entirely due to gas phase scattering [11]. The mass of the sample atoms affect the kinetic energies of the scattered primary ion and direct recoil-sputtered surface atoms, and the results will differ somewhat for other samples.

The peaks observed in Fig. 3 do not broaden, and the sharp onset on the short time of flight side of the peak which provides elemental identification of the surface species, does not shift for ambient pressures up to 3.6 mTorr. Similar results are obtained for all primary ion species and ambient gas combinations listed in Table I. Fig. 4 shows a set of DRS data for 10 keV Ar^+ incident on Au in an Ar ambient at pressures ranging from 6.45×10^{-5} Torr to 2.6×10^{-3} Torr. The backscattered primary signal occurs at ~5 microseconds, and the Au DRS signal appears at 14 microseconds. Once again, except for intensity, the peak shape is unaffected by the ambient gas environment.

Fig. 5 shows the ISS signal intensity as a function of pressure for 10 keV Ar^+, Ne^+ and He^+ in Ar, O_2, N_2, and H_2 ambients, and Fig. 6 shows the DRS intensities as a function of ambient pressure in the same gases. The ISS intensity was determined by summing all the counts under the peak as shown in Fig. 3. The DRS intensity was determined by integrating across the DR peak starting at the minumum between the elastic and DR peaks (e.g. 13 μsec in Fig. 4). The maximum pressure for hydrogen is limited by the poor compressibility (and consequently low pumping speed) of hydrogen, and the requirement of maintaining the pressure at the detectors $<2x10^{-5}$ Torr for safety reasons, rather than loss of signal due the hydrogen background. The usable hydrogen pressure range has been extended so that it matches that of the other gases by using a 70 l/sec turbomolecular pump in series with the 60 l/sec pumps connected to the detector chambers.

In each case, the data fit a straight line on a semi-log plot, corresponding to a constant effective cross section over the measured pressure range, in accord with Eq. 7. The slope Λ of the plots in Figs 5 and 6 is related to the cross sections $<\sigma>$, σ_1 and σ_2 by

$$\Lambda = -(d_1 \sigma_1 + d_2 \sigma_2)/kT = - (d1+d2) < \sigma>/kT \qquad (9)$$

in accord with eqs. 6 and 7, and

$$\sigma_2 = (\Lambda kT - d_1 \sigma_1)/d2 \qquad (10)$$

The experimentally determined mean collisional cross sections $<\sigma>$ for 10 keV primary ions in various gases for ISS and DRS are listed in Table 1.

In order to obtain σ_1 and σ_2 from the measured value of $<\sigma>$, the DRS detector was moved to a position directly opposite the ion beam line. Fig. 7 shows a high resolution scan of a 10 keV Ne^+ primary ion beam for Ar ambient gas pressures ranging from 0.1 to 0.72 Pa ($7.75x10^{-4}$ to $5x10^{-3}$ Torr). The ion pulse is very nearly symmetric, with a half width of ~160 nsec, independent of the background gas pressure. The time resolution is limited by the frequency of the dynamically variable clock rate [10] (which in this case was 25 MHz) to 40 nsec. The beam current rise time is only slightly longer than one tick of the clock, while the fall is somewhat slower, with a reasonably stable near-flat top with a duration of ~120 nsec resulting from the unique manner in which the dual-deflection system [10] produces the pulsed ion beam. The lack of broadening in the primary ion pulse is directly responsible for the well-defined rise and constant peak shape manifested in the data of Figs. 3 and 4.

Fig. 8 shows the primary ion beam peak intensity as a function of ambient pressure for Ar^+, Ne^+ and He^+ beams in Ar, O_2, N_2 and H_2. Since the count rate was very high, only the height of the peak was used in plotting Fig. 8. The attenuation of the primary ion beam count rate

with increasing pressure now results only from attenuation of the incoming beam by gas phase collisions, and therefore corresponds to σ_1 where

$$\sigma_1 = \Lambda\, kT\, /d \qquad (11)$$

and d=0.330 m is the distance between the last aperture in the ion beam line and the entrance to the differentially pumped detector in the modified configuration. The resulting values of σ_1 and σ_2 are shown in Table I. The cross section values corresponding to the data of Figs. 5-7 represent the signal collected in a very small solid angle and do not necessarily correspond to the total scattering cross section. Nevertheless, comparing our value for e.g. the 10 keV Ar^+/Ar signal attenuation (σ_1=6.65x10^{-20} m^2), with the Ar^+/Ar momentum transfer cross section of Phelps [12], (momentum transfer cross section=2.88x10^{-19} m^2), we find satisfactory agreement.

In order to define the maximum pressure at which ToF-ISARS may be used for surface characterization, we must define a "minimum acceptable" signal-noise ratio, or equivalently, the largest signal attenuation consistent with the acquisition of usable data. For a given geometric configuration, the signal:noise ratio depends on the solid angle subtended by the detector, average beam current, and data collection time. It should be borne in mind that an increased count rate resulting from an increase in the detector solid angle is purchased at the price of decreased mass resolution. The 1 mm diameter differential pumping apertures depicted in Fig. 1 were chosen to provide maximum differential pumping ratio, while imposing little or no reduction in the number of particles which strike the 1 cm diameter channeltron electron multipliers located at a distance of 0.7 m, and subtending a solid angle of 2x10^{-4} sr.

In order to do meaningful surface analysis, the ion beam dose should not be so large that the analyzed surface is damaged by the ion beam. The data presented here were typically acquired using an average ion beam current of 5x10^{-10} amps with a 30-40 second data acquisition time. The corresponding beam dose is ~1x10^{11} ions per spectrum. The beam is typically rastered over an area of 4x10^{-6} m^2 (2 mm square). For normal incidence ISS, the dose is therefore 2.5 x 10^{16} ions/m^2.(2.5x10^{12} ions/cm2), compared with a value of 1x10^{19} atoms/m^2 (1x10^{15} atoms/cm^2) present at the surface of a typical solid. For DRS, which requires glancing incidence, the dose is approximately 10x lower. These doses are low enough to ensure that the analyzed surface is not modified by the analysis process.

The typical signal/noise ratio of a spectrum acquired under vacuum conditions is ~100:1-150:1. As the signal intensity decreases with increasing ambient pressure, the signal:noise ratio decreases approximately as the square root of the total number of counts, limited by the electron multiplier dark count of 1-2 counts per histogram bin. For Ar^+ in an Ar ambient (Fig. 9), the signal:noise ratio decreases to ~3:1 at a pressure of 0.8 Pa. At this pressure, the signal has decreased by a factor of ~ 3000 and the signal:noise ratio has decreased by a factor of 50-60.

Figs. 10 and 11 summarize the calculated variation in signal intensity for ISS (Fig. 10) and DRS (Fig. 11), based on the σ_1 and σ_2 cross section values in Table I. Similar data can be generated for systems of arbitrary geometry using these cross section values and eq. 6. The dashed horizontal lines correspond to signal attenuation by a factor of 10^3, a somewhat conservative estimate of the minimum usable signal, and a more optimistic 10^4 attenuation factor. Because of the exponential dependence of the signal on the background pressure, the 10-fold variation between the "conservative" and the "optimistic" limits corresponds to a relatively small shift in the estimated maximum ambient pressure.

For ISS, the "usable pressure range" indicated by the upper horizontal dashed line ranges from 0.45 to 1.8 Pa ((3.4-13.5 mTorr). The highest usable pressures are achieved for low M_1/M_2 ratios, while high M_1/M_2 ratios correspond to low maximum ambient pressures. This result may be understood by reference to the theory of particle stopping in solids [13-15]. The maximum projected ranges correspond to light projectiles in a sample with heavy target atoms. Conversely, heavy projectiles produce very dense collision cascades and consequently have relatively short projected ranges. For ISS, the kinetic energy of the primary ion is different before and after collision with the surface, but the mass of the energetic particle does not change. For DRS (Fig. 11), both the mass and the kinetic energy of the outgoing particles differ from those of the primary ion, and the variation of the resulting maximum pressure (0.8-2.3 Pa (6-17.3 mTorr)) is not so simply related to the masses of the primary ions and target atoms. By decreasing the chamber dimensions, the maximum pressure can be proportionately increased up to a practical limit of approximately 10x the values shown in Figs. 10 and 11 [16].

SUMMARY.

In order to demonstrate the utility of pulsed ion beam surface analytical techniques in ambient gas environments, we have measured the ISS and DRS signal attenuation for a stabilized clean surface as a function of ambient gas pressure using a variety of ion beam and back filled gas species. No peak shift is observed from vacuum up to the maximum pressures tested. The signal attenuation is interpreted in terms of a mean free path and corresponding momentum transfer cross section. The effective cross section for an ISS or DRS signal is deconvoluted into two components consisting of (1) scattering between the primary beam and the ambient gas prior to collision with the sample, and (2) scattering between the outgoing particle (scattered primary ion or direct recoil-sputtered surface atom) and ambient gas. The two cross section values (σ_1 and σ_2) may be used to calculate anticipated performance of an ion beam surface analysis system of arbitrary geometry in an ambient gas environment.

When a second turbomolecular pump is used in series with the pumps on the detector chambers. the maximum ambient pressure is determined by signal attenuation at high pressures, rather than the operating limits of the channel electron multipliers. By proper design of the differential pumping apertures, it is possible to achieve ambient gas surface analysis without sacrificing signal. The maximum ambient gas pressure for which such analysis may be performed using a 10 keV ion beam is 0.45-2.3 Pa (3-17 mTorr), depending on the ion beam-ambient gas combination. The mass dependence of this variation in maximum pressure can be explained in terms of the theory of energetic particle stopping in solids. By reducing the chamber volume, the maximum pressure at which surface analysis may be performed could be raised to a practical limit of 25-50 Pa (0.22-0.44 Torr). The small chamber volume (2-4 cm diameter) would be suitable for in situ studies of gas-surface chemical reactions but would severely limit processes such as thin film deposition which require larger working volumes.

REFERENCE

1. A. R. Krauss, O. Auciello, Y. Lin, R. P. H. Chang and D. M. Gruen, Integrated Ferroelectrics 8, 129 (1995)
2. O. Auciello, A. R. Krauss and K. D. Gifford, in Ferroelectric Thin Films, Synthesis and Basic Properties, ed. by C.A.P. Araujo, J. F. Scott and G. W. Taylor, Gordon and Breach, in press
3. D. P. Smith, J. Appl. Phys. **38**, 340 (1967)
4. L. Marchut, T. M. Buck, G. H. Wheatley and C. J. McMahon, Surf. SCi. **90**, 635 (1979)
5. M. Aono, Nucl. Instrum. Meth. Phys. Res. **B2**, 374 (1984); M. Katayama, E. Nomura, N. Kanakama, H. Soejima, and M. Aono, Nucl. Instrum. Meth. Phys. Res. **B33**, 857 (1988)
6. H. Niehus and G. Comsa, Nucl. Instrum. Meth. Phys. Res. **B15**, 122 (1986); H. Niehus, Surf. Sci. **166**, L107 (1986)
7. J. W. Rabalais, Science **250**, 521 (1990)
8. K. Eipers, K. Waters and J. A. Shultz, J. Amer. Ceram. Soc. **76**, 284 (1993)
9. A. R. Krauss, M. Rangaswamy, Y. Lin, D. M. Gruen, J. A. Schultz, H. K. Schmidt and R. P. H. Chang, in "Multicomponent and Multilayered Thin Films for Advanced Micro-technologies" O. Auciello and J. Engemann eds Kluwer Academic Publishers (1993), 251
10. A. R. Krauss, Y. Lin, O. Auciello, G. J. Lamich, D. M. Gruen, J. A. Schultz and R. P. H. Chang, J. Vac, Sci, Technol. **A12**, 1943 (1994).
11. Y. Lin , A.R. Krauss. O. Auciello, Y. Nishino, D.M. Gruen, R. P. H. Chang, and J.A. Schultz, J. Vac. Sci. Technol., **A12** , 1557 (1994)
12. A.V. Phelps, J. Phys. Chem. Ref. Data. **20**, 557 (1991)
13. J. Lindhard, V. Nielsen, and M. Scharff, Mat. Fys. Kongl. Dansk. Vid. Selskab **36**, 1 (1968)
14. J. Lindhard, M. Scharff and H. E. Schiott, Mat. Fys. Kongl. Dansk. Vid. Selskab **33**, 14 (1968) 1
15. J. Lindhard, V. Nielsen, M. Scharff, and P. V. Thomsen, Mat. Fys. Kongl. Dansk. Vid. Selskab **33,10**, 1 (1968) 1
16. H. K. Schmidt, J. A. Schultz and Z. Zheng in Diamond and Diamond-like Coatings, R. E. Clausing ed, (Plenum Press, New York) 1991, p. 669

Table 1. The experimentally determined collisional cross section of ISS and DRS for various gases exposed to 10 kev Ar^+, Ne^+ and He^+ beams.

Mode	Primary ion	Gas	$<\sigma>$ (m^2)	σ_1 (m^2)	σ_2 (m^2)
ISS	Ar^+	Ar	1.03×10^{-19}	6.65×10^{-20}	1.96×10^{-19}
		O_2	1.38×10^{-19}	6.62×10^{-20}	3.21×10^{-19}
		N_2	1.04×10^{-19}	7.32×10^{-20}	1.82×10^{-19}
		H_2	9.32×10^{-20}	3.55×10^{-20}	2.40×10^{-19}
	Ne^+	Ar	4.64×10^{-20}	2.49×10^{-20}	9.81×10^{-20}
		O_2	6.18×10^{-20}	5.16×10^{-20}	8.65×10^{-20}
		N_2	5.18×10^{-20}	3.84×10^{-20}	8.39×10^{-20}
		H_2	7.05×10^{-20}	1.16×10^{-20}	2.12×10^{-19}
	He^+	Ar	4.41×10^{-20}	2.43×10^{-20}	9.45×10^{-20}
		O_2	5.60×10^{-20}	4.57×10^{-20}	8.29×10^{-20}
		N_2	4.96×10^{-20}	3.57×10^{-20}	8.50×10^{-20}
		H_2	8.01×10^{-20}	6.72×10^{-20}	1.13×10^{-19}
DRS	Ar^+	Ar	8.17×10^{-20}	6.65×10^{-20}	1.18×10^{-19}
		O_2	1.44×10^{-19}	6.62×10^{-20}	3.32×10^{-19}
		N_2	1.43×10^{-19}	7.32×10^{-20}	3.11×10^{-19}
		H_2	9.42×10^{-20}	3.55×10^{-20}	2.36×10^{-19}
	Ne^+	Ar	3.09×10^{-20}	2.49×10^{-20}	4.55×10^{-20}
		O_2	4.25×10^{-20}	5.16×10^{-20}	2.04×10^{-20}
		N_2	4.37×10^{-20}	3.84×10^{-20}	5.63×10^{-20}
		H_2	N/A	1.16×10^{-20}	N/A

Figure Captions

Fig. 1 Differentially pumped ToF-ISARS thin film deposition and in situ surface analysis chamber.

Fig. 2 Detail of the differential pumping geometry.

Fig. 3 ISS spectra for 10 keV Ne^+ primary ions incident on a clean gold surface in various ambient argon pressures.

Fig. 4 DRS spectra for 10 keV Ar^+ primary ions incident on a clean gold surface in various ambient argon pressures.

Fig. 5 Integrated intensity of the ISS Au peak for 10 keV Ar^+ (5a), Ne^+ (5b), He^+ (5c), primary ions as a function of ambient gas pressure.

Fig. 6 Integrated intensity of the DRS Au peak for 10 keV Ar^+ (6a) and Ne^+ (6b) primary ions as a function of ambient gas pressure. The Au direct recoil sputtering yield for He^+ primary ions was too low to provide a complete data set.

Fig. 7 High resolution spectrum of a 10 keV primary Ne^+ ion beam directed directly into the DRS detector. The peak shape and width are unaltered by the ambient Ar.

Fig. 8 Peak intensity of the pulsed 10 keV primary ion beam (Ar^+ (8a), Ne^+ (8b) and He^+ (8c)), directed into the repositioned DRS detector as a function of ambient gas pressure.

Fig. 9 ISS spectrum for Ar^+ ion beam incident on gold in an O_2 ambient pressure of 6 mTorr.

Fig. 10 Calculated ISS I/Io values for Ar^+, Ne^+ and He^+ primary ions in an ambient gas environment of Ar, O_2, N_2 and H_2 as a function of ambient gas pressure. The two dashed horizontal lines define the upper and lower bounds of the region for which the signal:noise ratio approaches unity for the ion beam current and data acquisition times employed in the experiment.

Fig. 11 Calculated DRS I/Io values for Ar^+, Ne^+ and He^+ primary ions in an ambient gas environment of Ar, O_2, N_2 and H_2 as a function of ambient gas pressure. The two dashed horizontal lines define the upper and lower bounds of the region for which the signal:noise ratio approaches unity for the ion beam current and data acquisition times employed in the experiment.

Differentially Pumped ToF-ISARS Thin Film Deposition & In Situ Surface Analysis Chamber

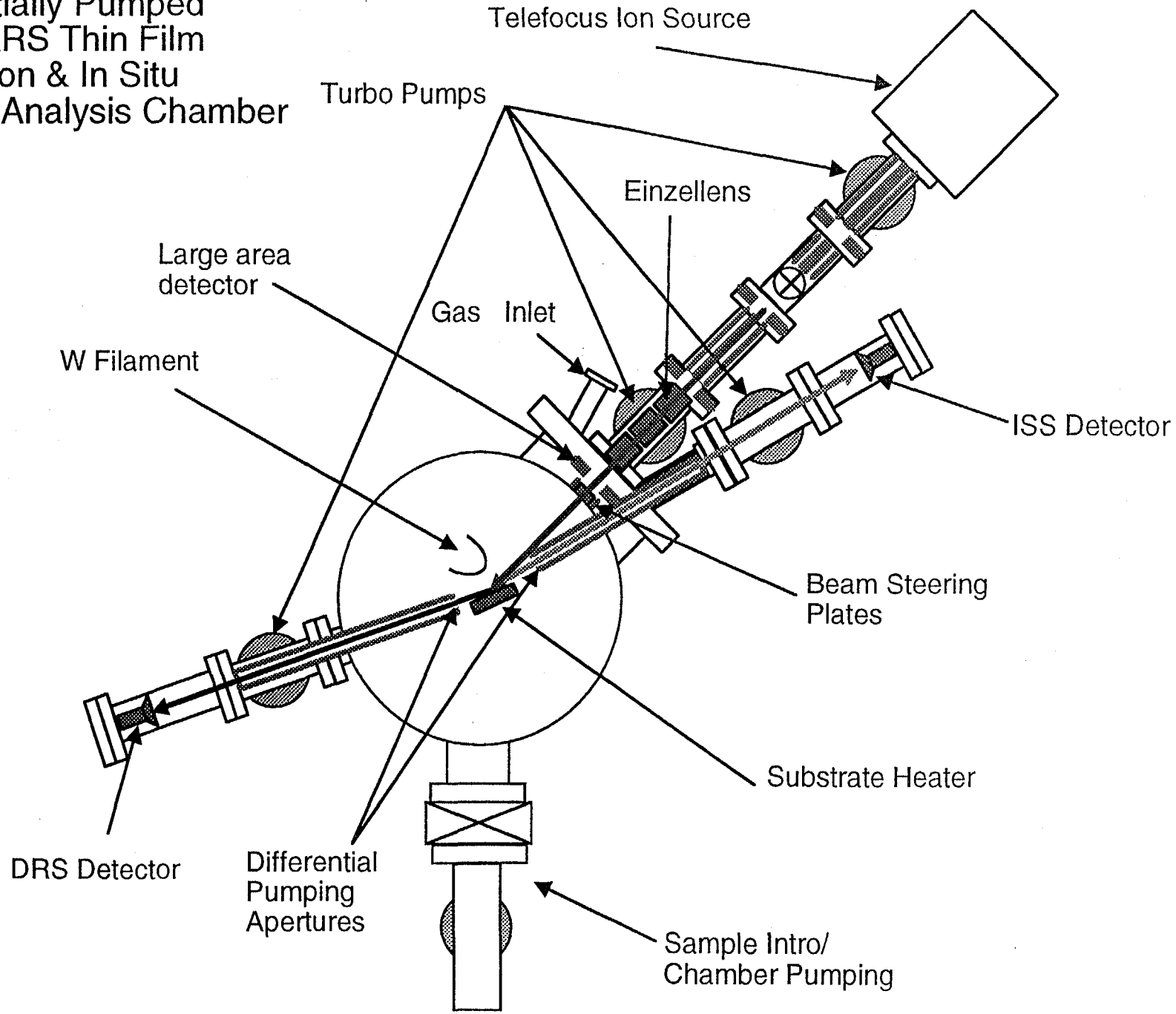

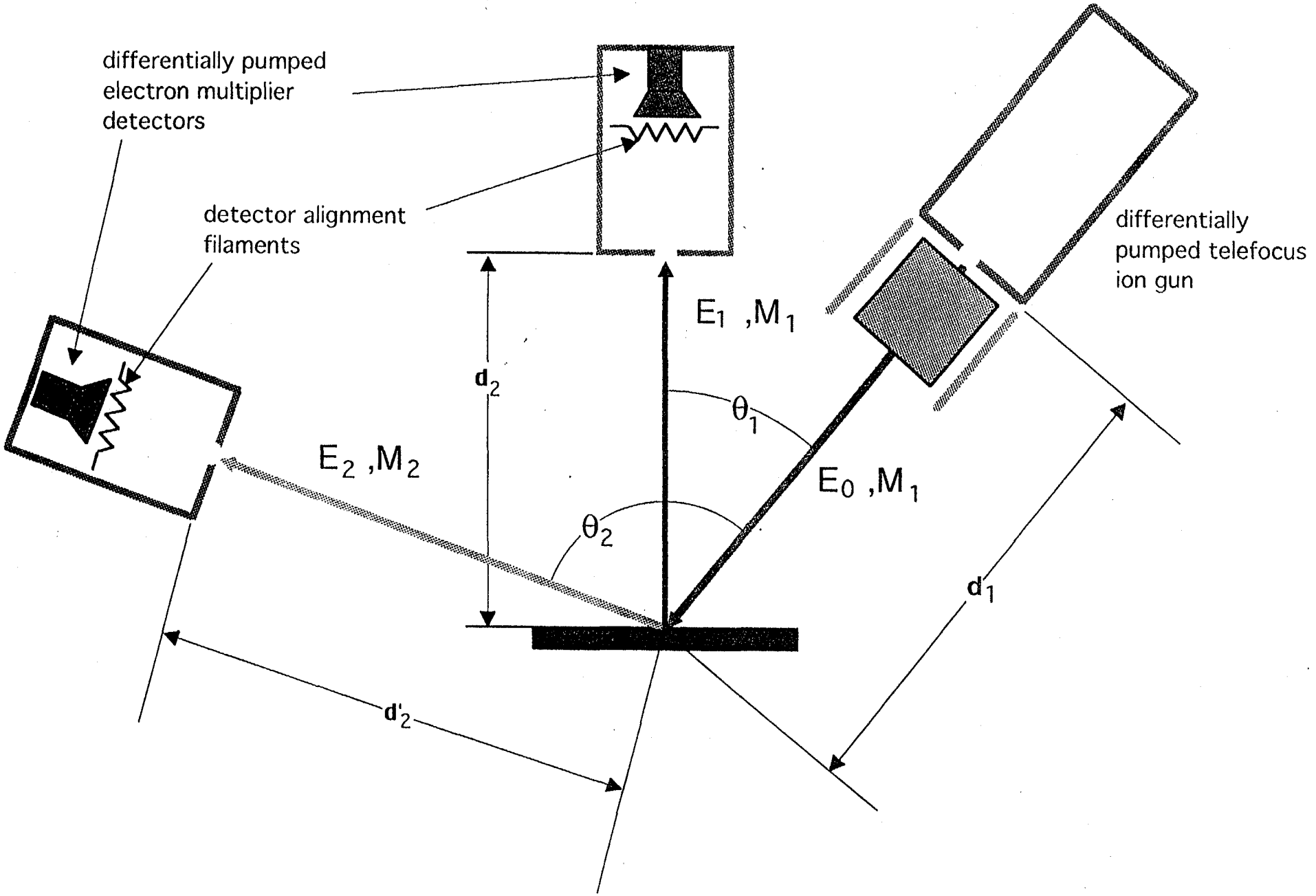
differentially pumped
electron multiplier
detectors
detector alignment
filaments
differentially
pumped telefocus
ion gun
E1 ,M1
d2
θ1
E2 ,M2
E0 ,M1
θ2
d1
d'2

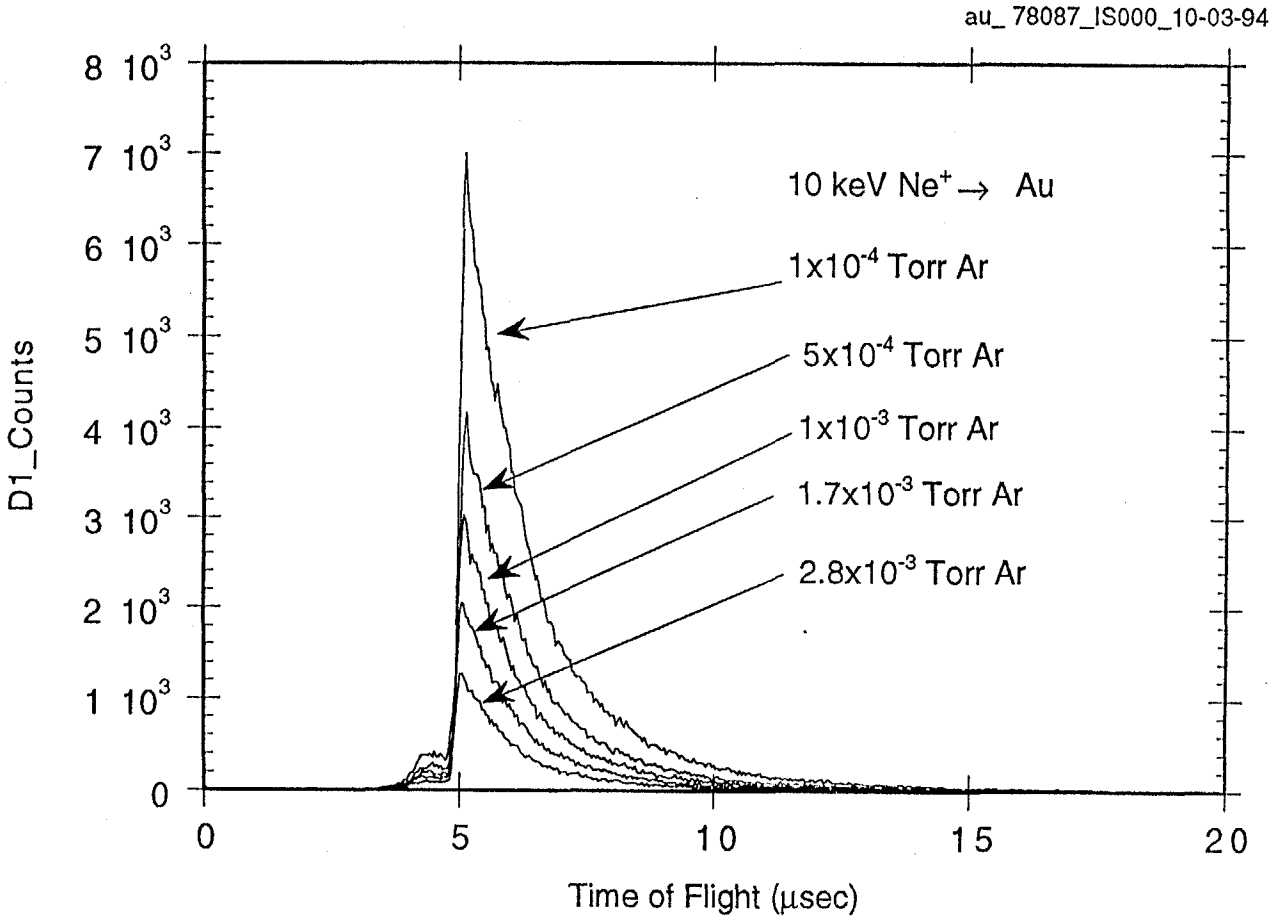
au_ 78087_IS000_10-03-94
8 10^3
7 10^3
6 10^3
5 10^3
4 10^3
3 10^3
2 10^3
1 10^3
0
D1_Counts
10 keV Ne+ → Au
1x10-4 Torr Ar
5x10-4 Torr Ar
1x10-3 Torr Ar
1.7x10-3 Torr Ar
2.8x10-3 Torr Ar
0
5
10
15
20
Time of Flight (µsec)

J. Im et al. Fig. 4

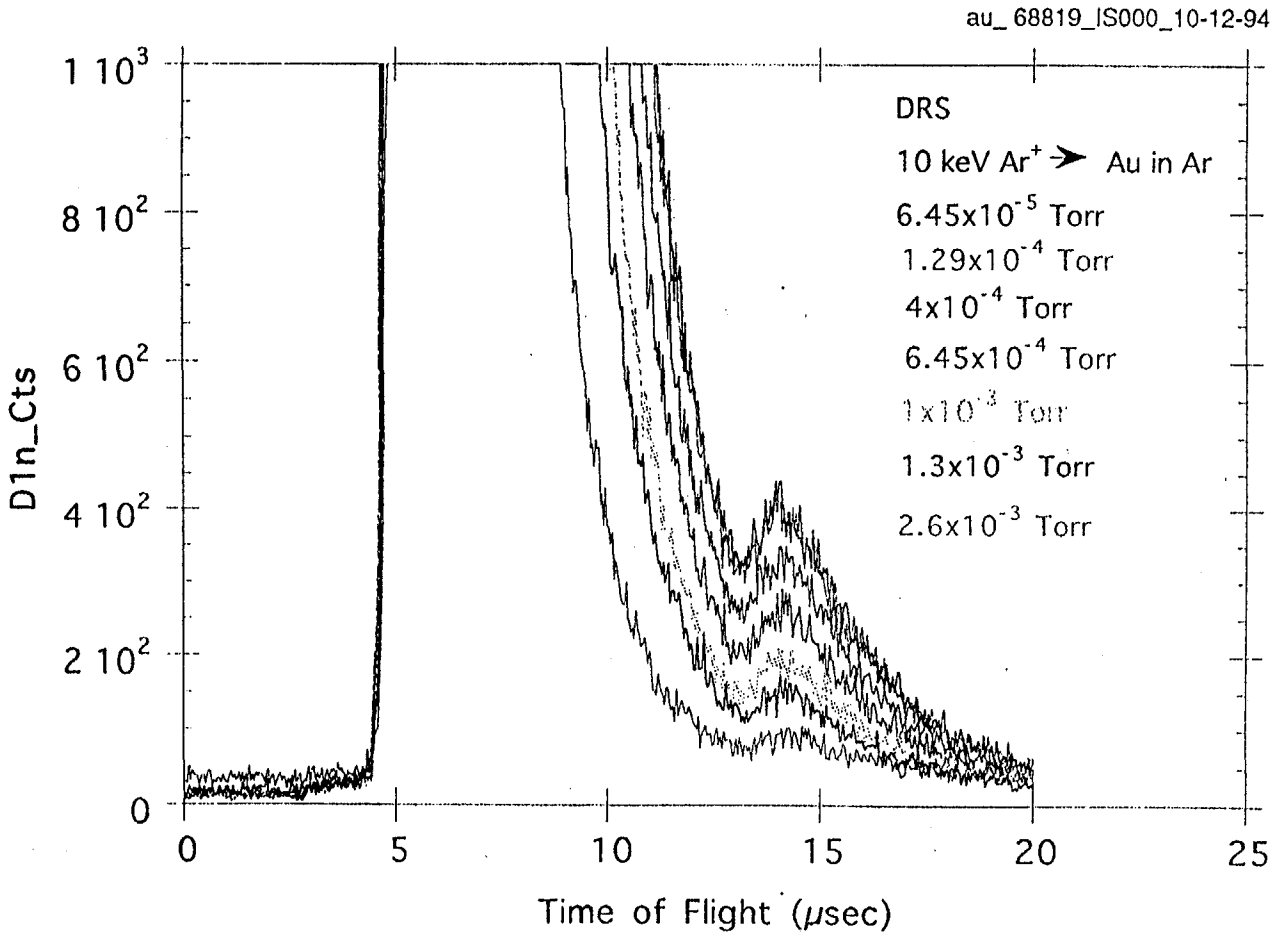

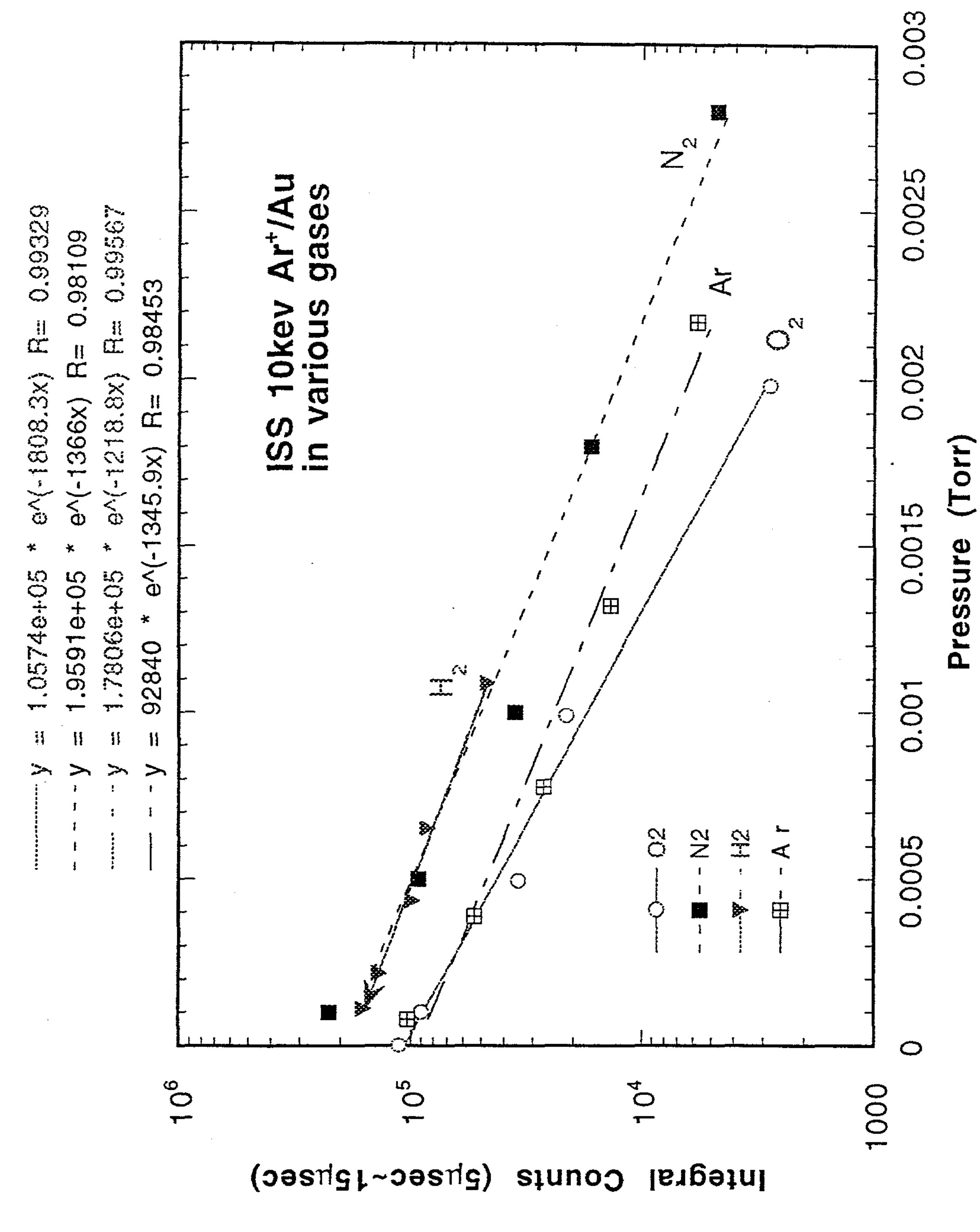

J. Im et. al. Fig. 5a

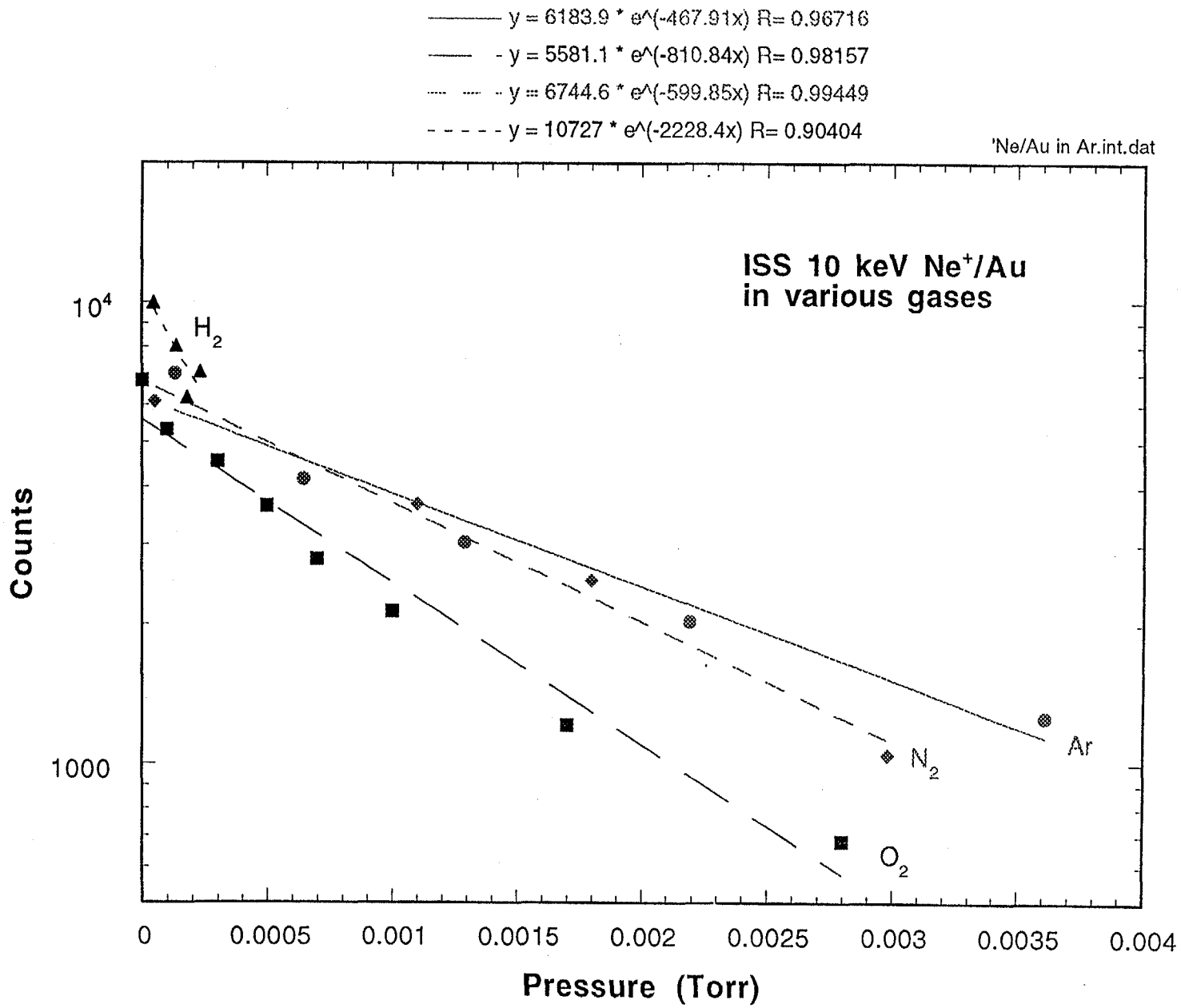

J. Im et al., Fig. 5b

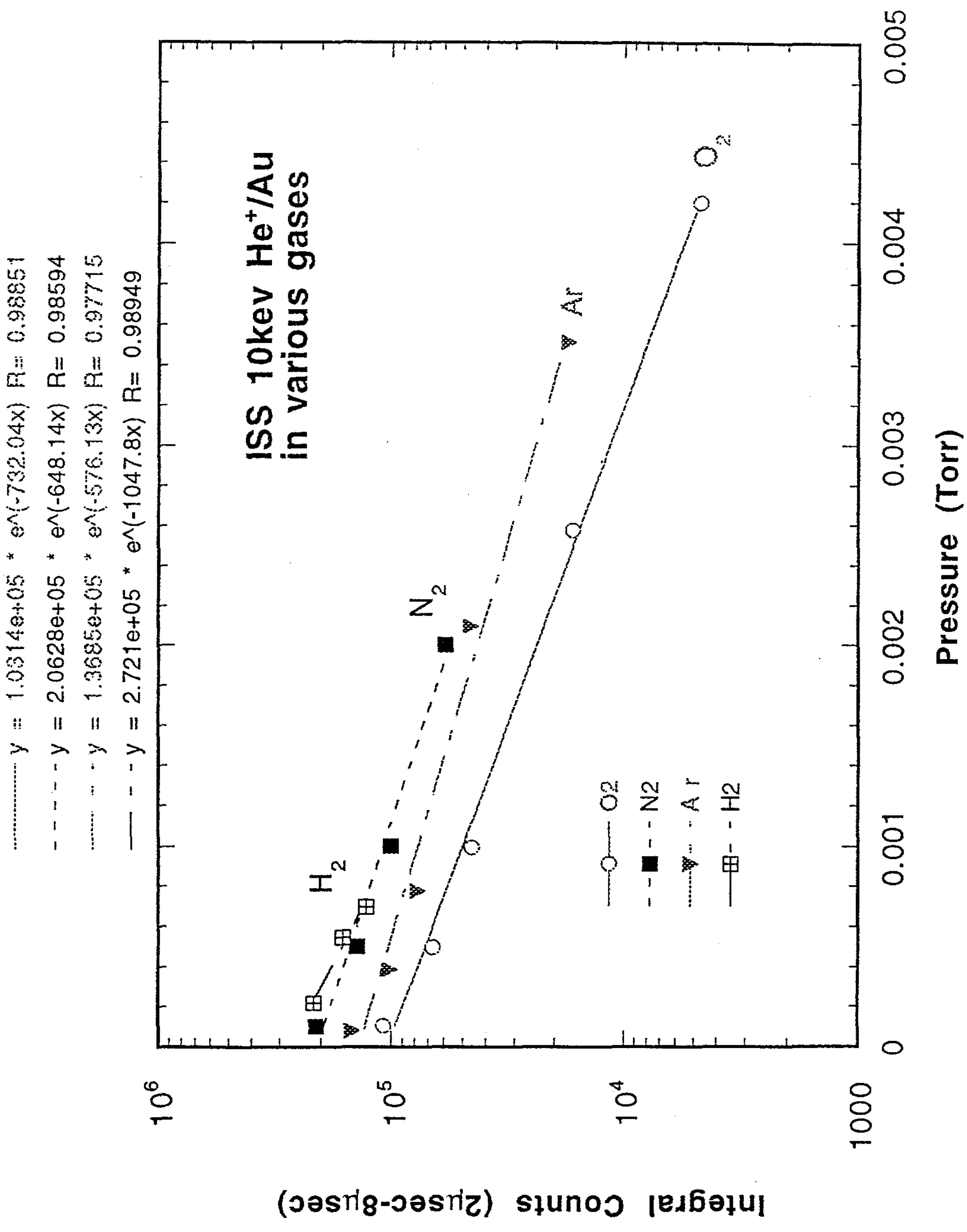

J. Im. et. al. Fig. 5C

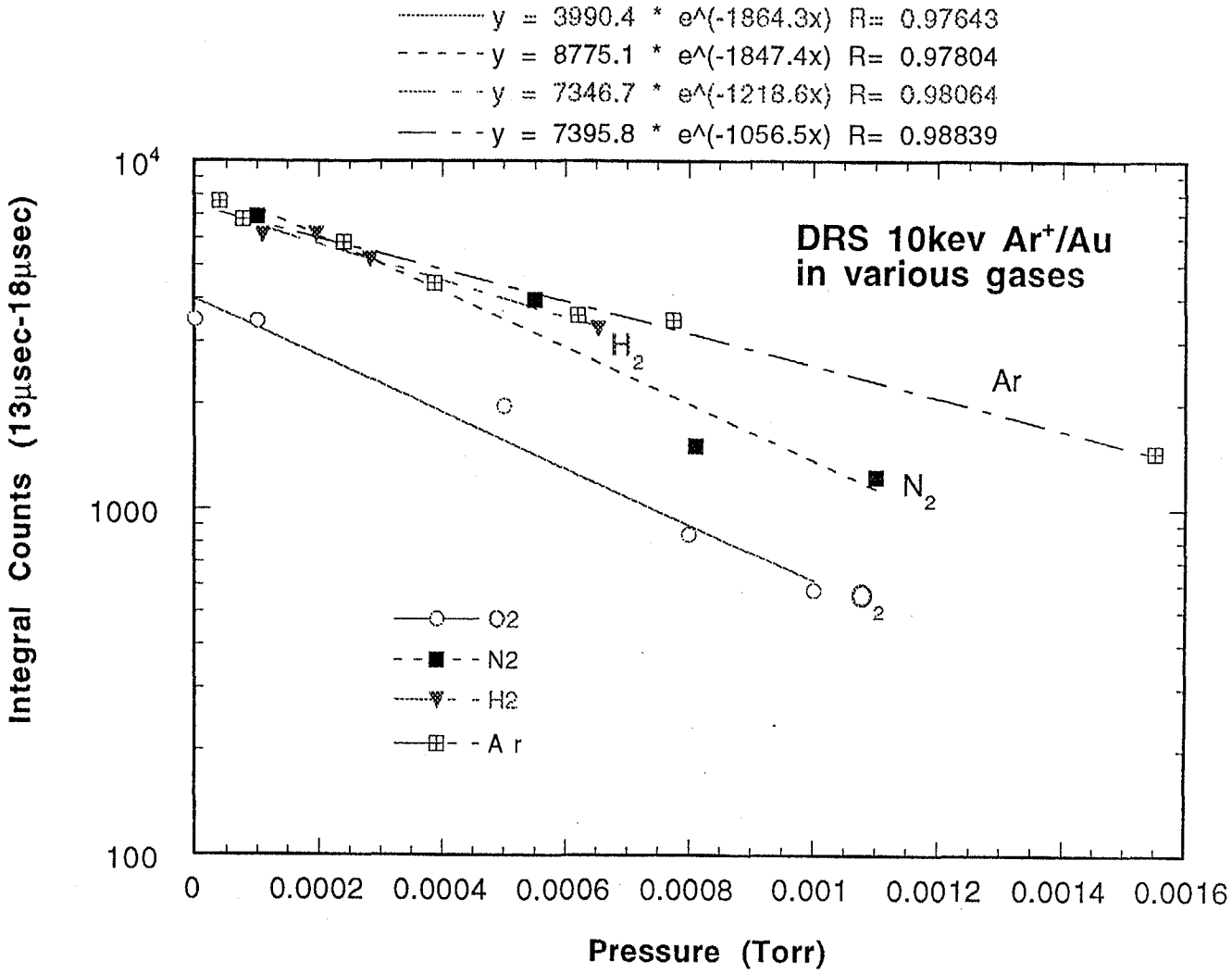

J. Im et al. Fig. 2

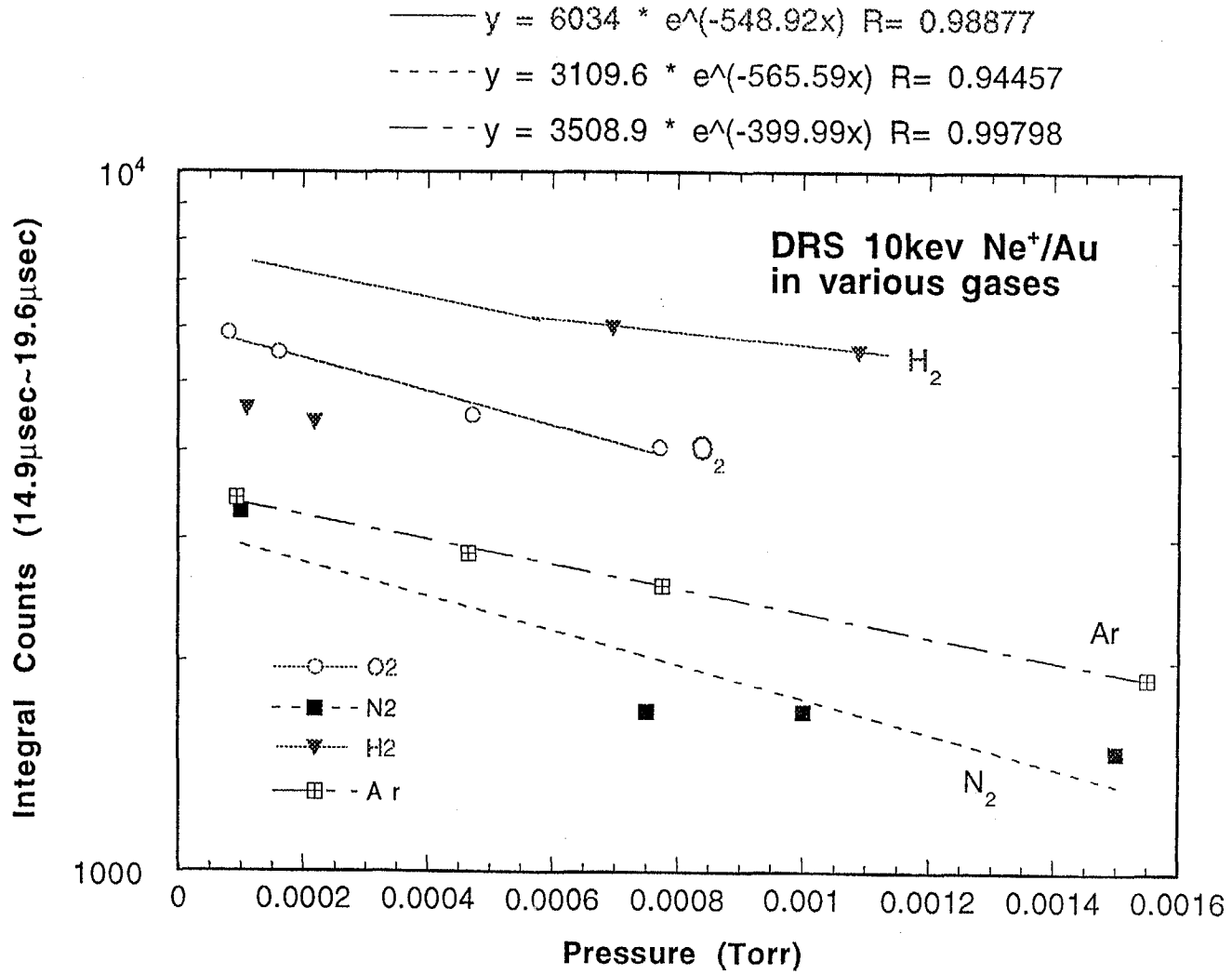

J. Im et al. Fig. 2

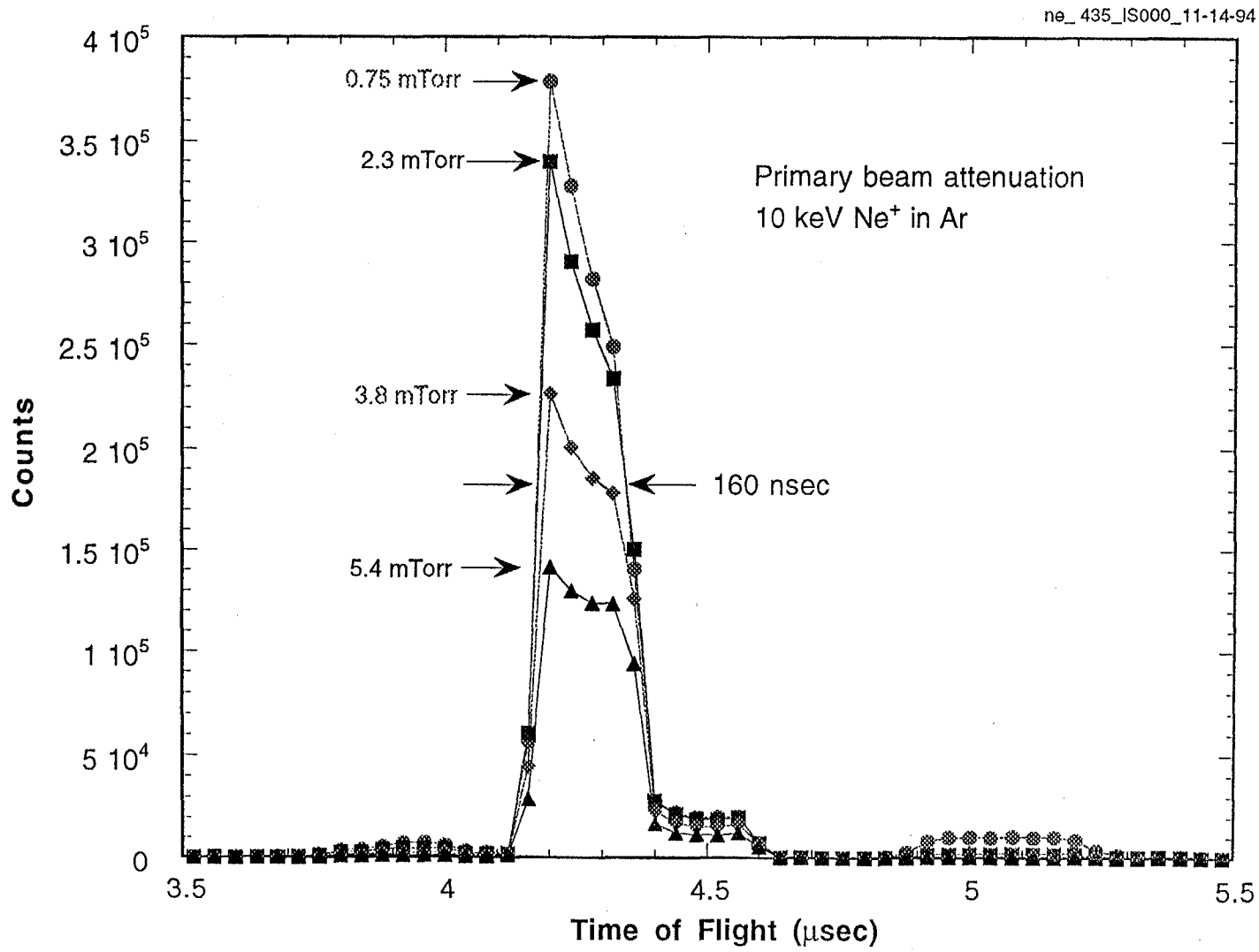

T. Tm et. al. Fig. 3

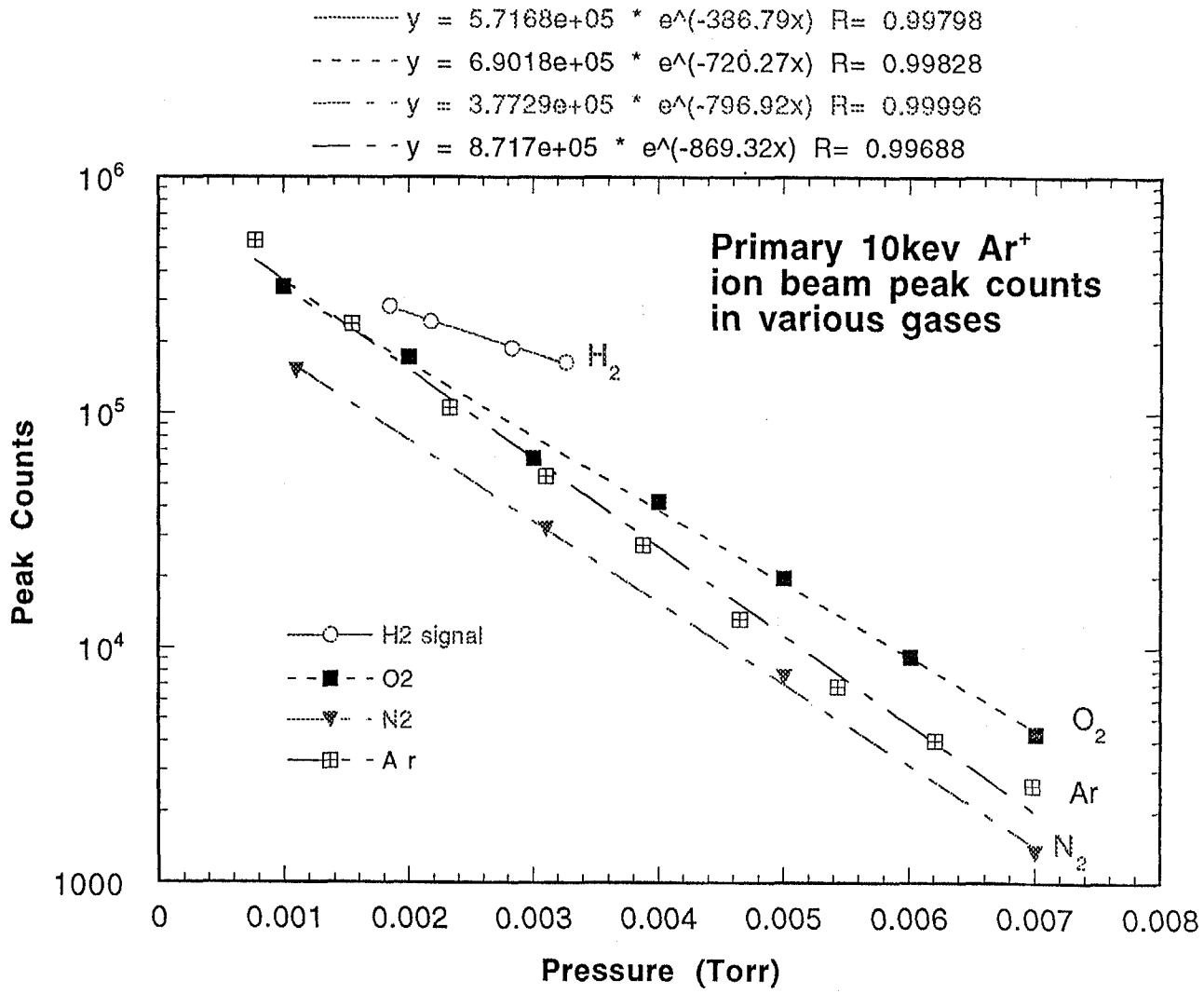
y = 5.7168e+05 * e^(-386.79x) R= 0.99798
y = 6.9018e+05 * e^(-720.27x) R= 0.99828
y = 3.7729e+05 * e^(-796.92x) R= 0.99996
y = 8.717e+05 * e^(-869.32x) R= 0.99688
Primary 10kev Ar+ ion beam peak counts in various gases
Peak Counts
Pressure (Torr)
H2 signal
O2
N2
Ar
H2
O2
Ar
N2
10^6
10^5
10^4
1000
0
0.001
0.002
0.003
0.004
0.005
0.006
0.007
0.008

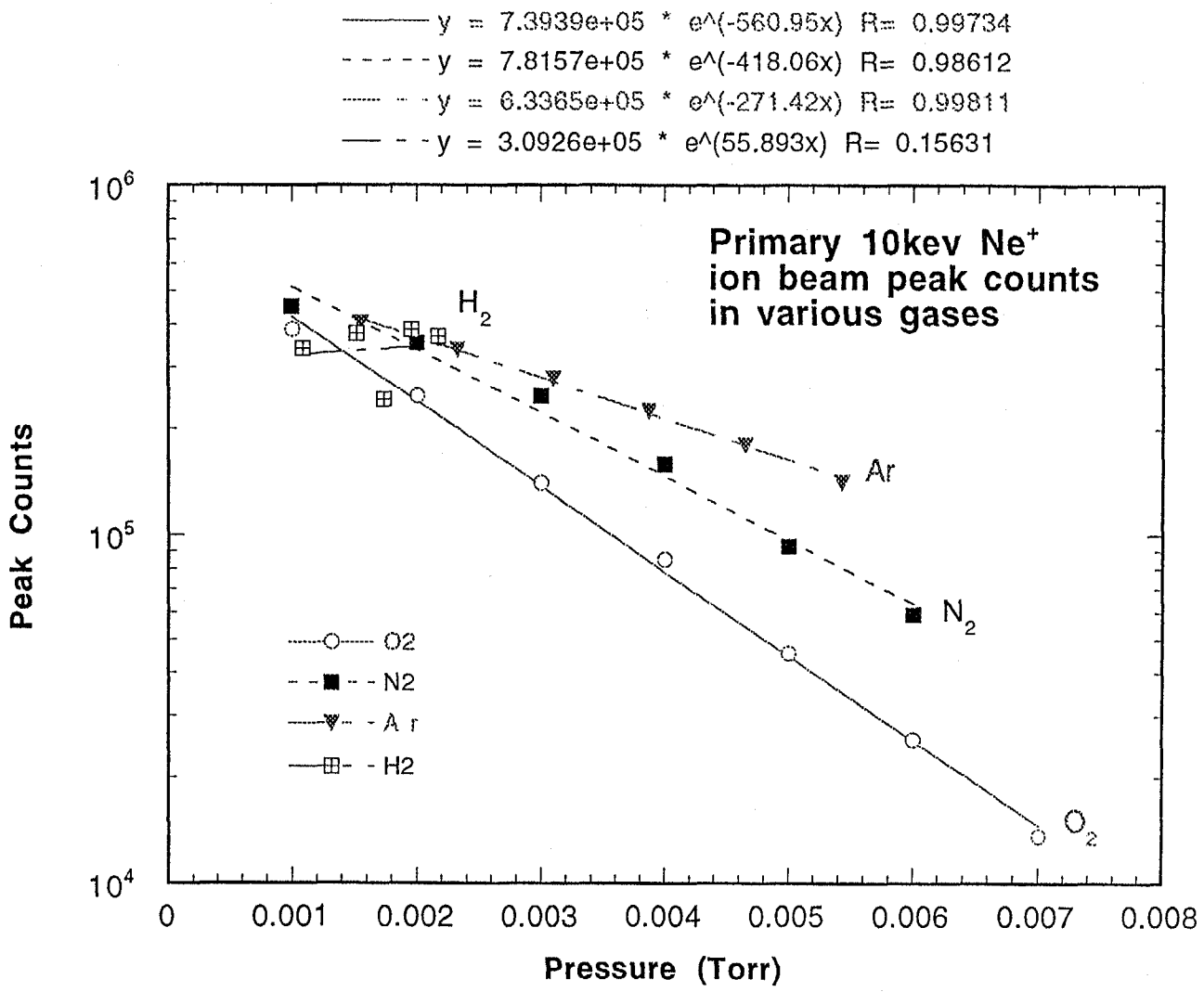

T. Im et al. Fig. 2b

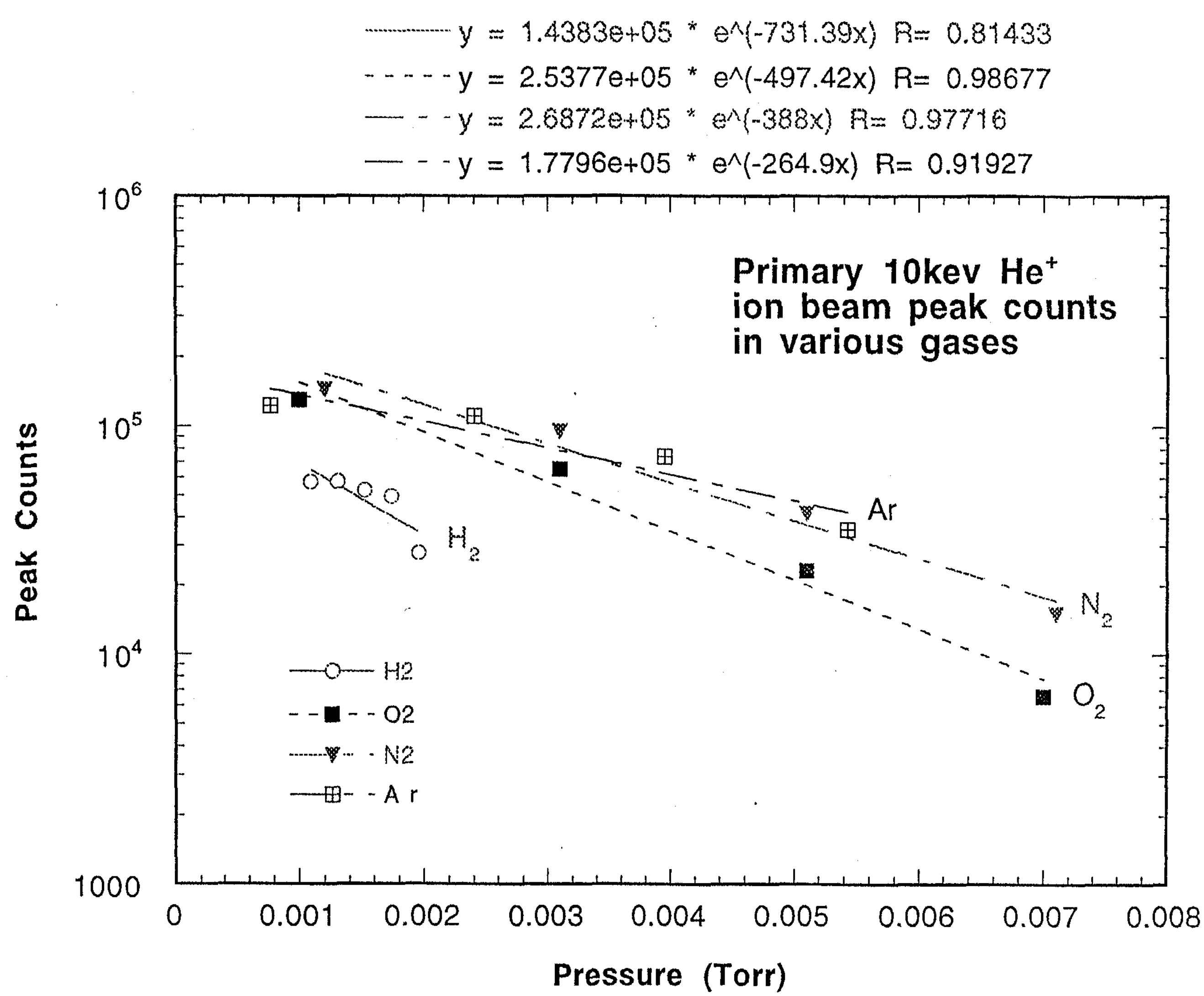

J. Im. et. al. Fig 7C

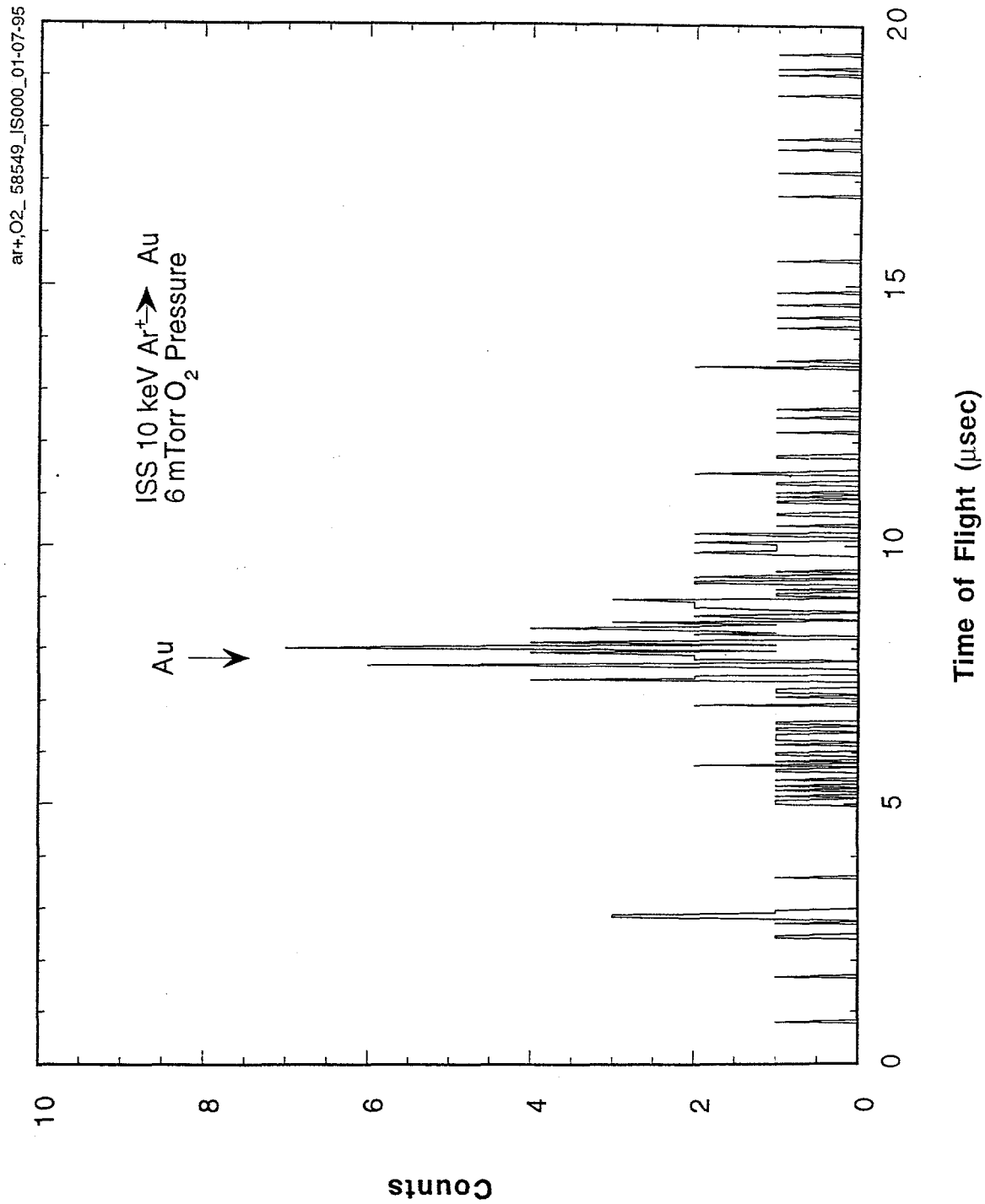

J. Im et al. Fig. 9

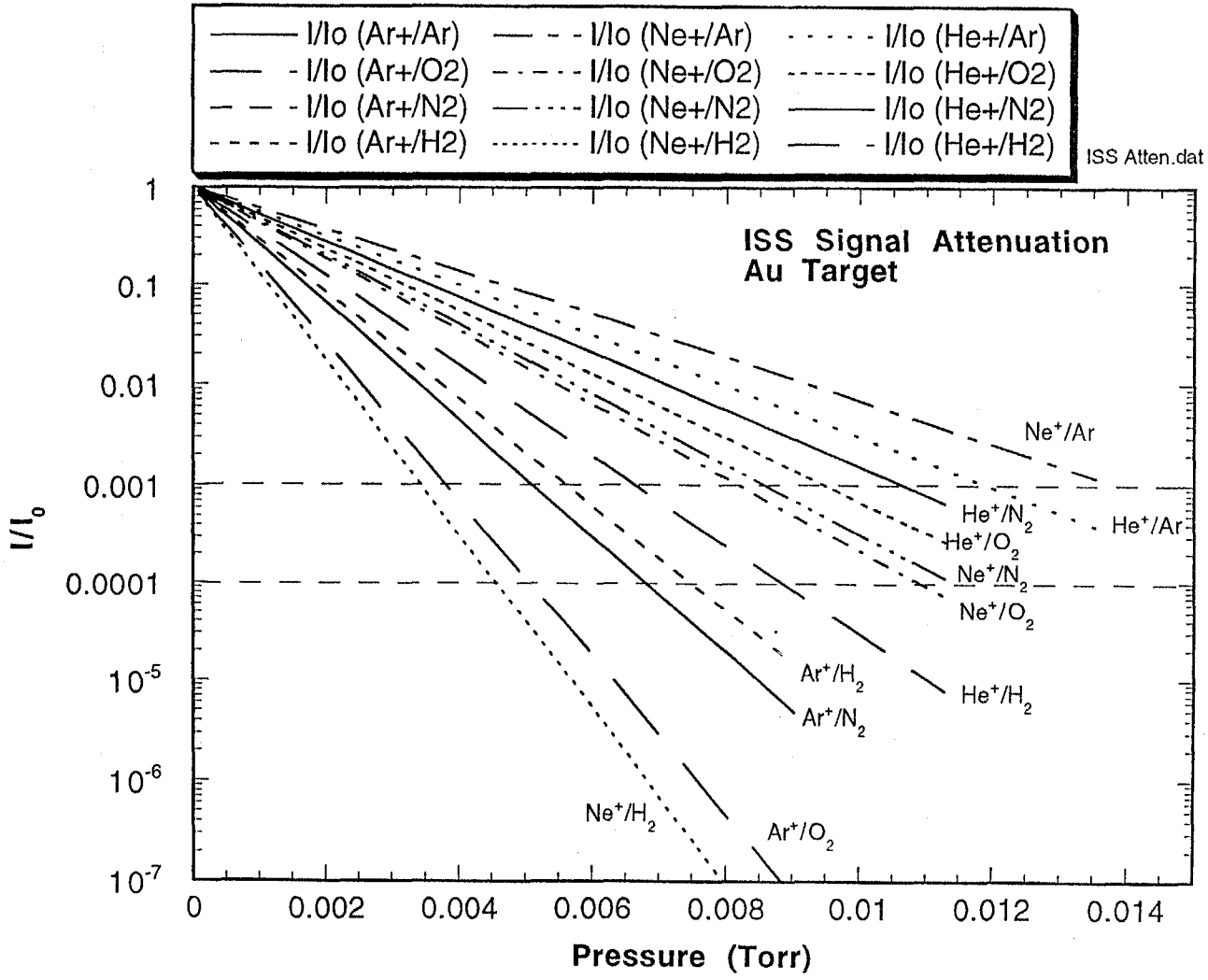
I/Io (Ar+/Ar)
I/Io (Ar+/O2)
I/Io (Ar+/N2)
I/Io (Ar+/H2)
I/Io (Ne+/Ar)
I/Io (Ne+/O2)
I/Io (Ne+/N2)
I/Io (Ne+/H2)
I/Io (He+/Ar)
I/Io (He+/O2)
I/Io (He+/N2)
I/Io (He+/H2)
ISS Atten.dat
ISS Signal Attenuation
Au Target
I/I0
1
0.1
0.01
0.001
0.0001
10-5
10-6
10-7
0
0.002
0.004
0.006
0.008
0.01
0.012
0.014
Pressure (Torr)
Ne+/Ar
He+/N2
He+/Ar
He+/O2
Ne+/N2
Ne+/O2
Ar+/H2
He+/H2
Ar+/N2
Ne+/H2
Ar+/O2

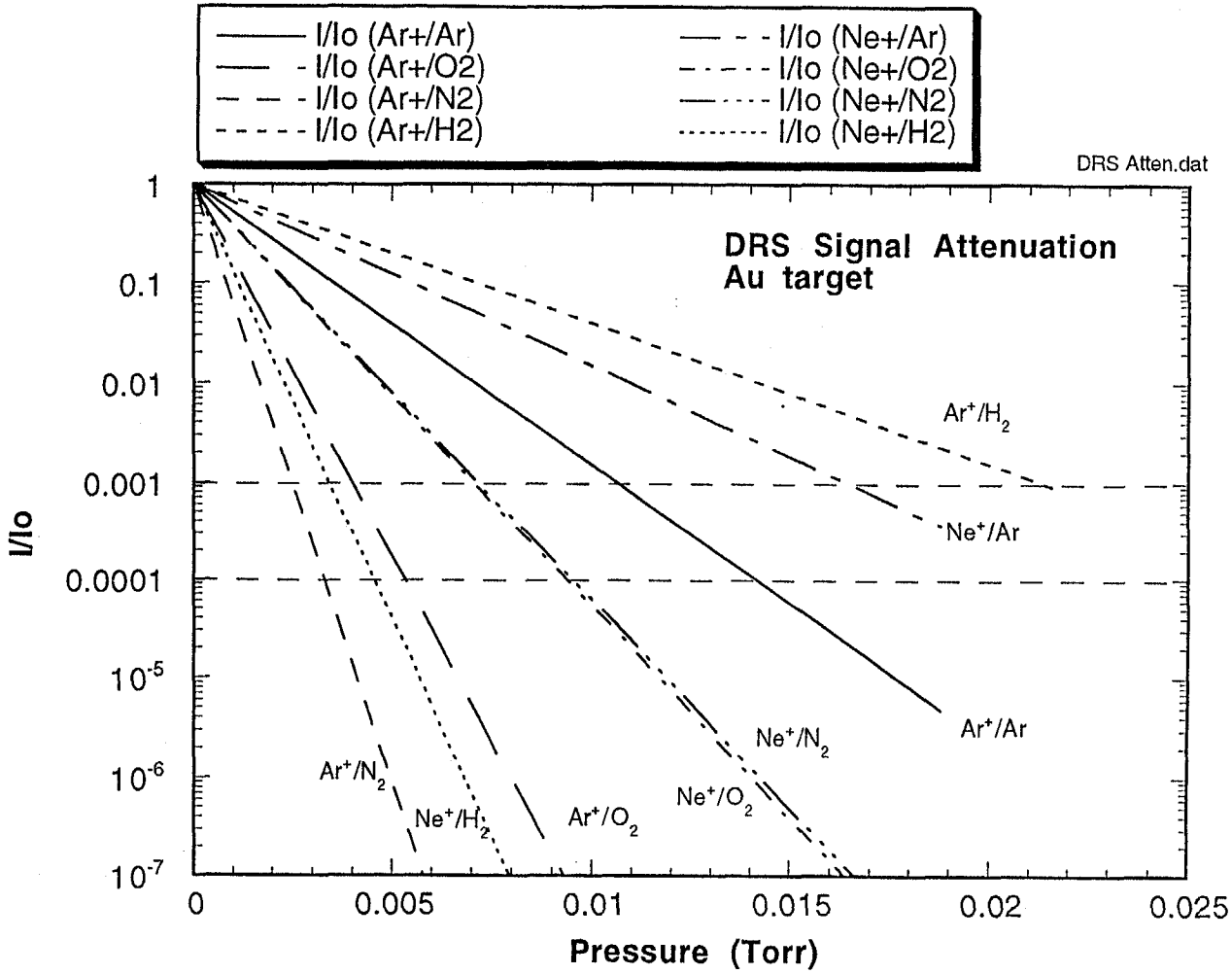

J. Im et.al. Fig. 11